JOURNAL OF GEOPHYSICAL RESEARCH, VOL. 113, C03028, doi:10.1029/2007JC004320, 2008

Observed and modeled meridional overturning circulation related flow into the Caribbean

Kerstin Kirchner,[1] Monika Rhein,[1] Christian Mertens,[1] Claus W. Böning,[2] and Sabine Hüttl[2,3]

Received 4 May 2007; revised 8 October 2007; accepted 4 December 2007; published 28 March 2008.

[1] A major pathway of the Atlantic meridional overturning circulation (MOC) is the warm inflow into the Caribbean Sea. The transport and the contribution of water from the South Atlantic is calculated from observations (ADCP data and hydrography) and compared to the results of the $\frac{1}{12}°$ FLAME model. The model and the observations show high consistency in the strength of the mean total inflow and its range of variability as well as in the general distribution of water from South Atlantic origin. The measurements give an annual mean South Atlantic Water (SAW) transport into the Caribbean of 9.3 Sv with high variability. This estimate has to be regarded as a lower bound since the present method (using temperature and salinity data) cannot identify the SAW included in the North Equatorial Current (NEC), which recirculated and was transformed in the interior tropical Atlantic. The model transport reproduces the observational values rather closely, with an annual mean inflow of 8.6 Sv and similar high variability. Closer inspection of the SAW pathways in the model suggest that the additional contribution by the NEC-pathway is only about 2 Sv. The model results confirm the relative importance of the MOC pathways suggested by observations: the Caribbean inflow seems to be the main pathway (63%) for the warm and central water ($\sigma_\theta < 27.1$ kg m^{-3}), whereas for the intermediate water a larger fraction (59%) is transported northward at the eastern side of the Lesser Antilles.

Citation: Kirchner, K., M. Rhein, C. Mertens, C. W. Böning, and S. Hüttl (2008), Observed and modeled meridional overturning circulation related flow into the Caribbean, *J. Geophys. Res.*, *113*, C03028, doi:10.1029/2007JC004320.

1. Introduction

[2] In the North Atlantic, the meridional overturning circulation (MOC) transports heat and salt from the South Atlantic into high latitudes, where cooling at the surface eventually induces vertical overturning and southward flow of cold deep water. The warm upper branch of the MOC, which transports South Atlantic Water (SAW) across the equator, is difficult to observe since the wind driven subtropical gyres and the complex equatorial current system interact with the SAW flow. The region north of the retroflection of the North Brazil Current (NBC) and south of the subtropical gyre (i.e., the North Equatorial Current, NEC) is one of the sparse locations suitable to directly observe the principal part of the net SAW flow. As an appropriate location the inflow into the Caribbean through the Lesser Antilles Islands (Figure 1) was chosen. Here, most of the water masses from the North and South Atlantic can be distinguished by their different temperature and salinity features [*Schmitz and Richardson*, 1991; *Poole and Tomczak*, 1999; *Rhein et al.*, 2005].

[3] The SAW is transported to the Caribbean by two mechanisms: at the NBC retroflection, large anticyclonic eddies containing SAW pinch off and move northwestward toward the Lesser Antilles [e.g., *Fratantoni and Glickson*, 2002; *Goni and Johns*, 2003]. Second, some studies suggest the existence of a coastal current, the Guyana Current, transporting SAW from the NBC along the coast toward the Caribbean Sea [*Lux et al.*, 2001; *Lumpkin and Garzoli*, 2005]. More recent results from moorings at the French Guiana shelf however negate a persistent Guyana current [*Baklouti et al.*, 2007]. The SAW flow is supplemented by Water from the North Atlantic, which is carried by the NEC into the Caribbean inflow region [*Snowden and Molinari*, 2003]. The water in the Caribbean Sea is therefore a mixture of southern and northern hemispheric waters.

[4] In the work of *Rhein et al.* [2005] CTD, vessel mounted Acoustic Doppler Current Profiler (ADCP), and lowered ADCP (LADCP) measurements taken in 2000–2004 were used to estimate transports of South Atlantic Water (SAW) through the Caribbean passages south of Guadeloupe (Figure 1) and across 16°N at the Atlantic route (eastward of the Caribbean island arc). They showed that the Caribbean inflow is the main pathway for upper

[1] Institut für Umweltphysik, Universität Bremen, Bremen, Germany.
[2] Leibniz Institut für Meereswissenschaften an der Universität Kiel (IFM-GEOMAR), Kiel, Germany.
[3] Now at Institut für Umweltphysik, Universität Bremen, Bremen, Germany.

0148-0227/08/2007JC004320$09.00

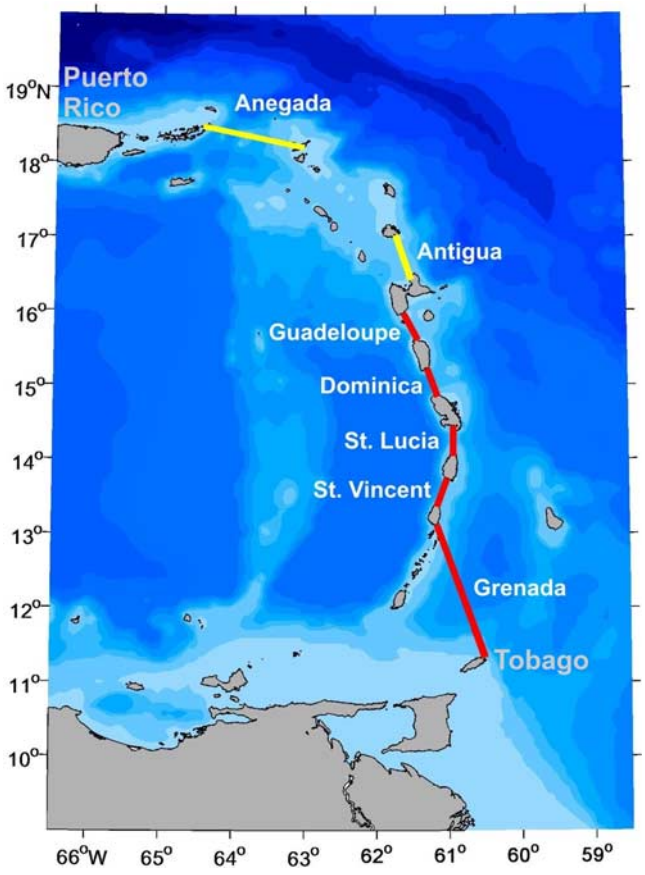

Figure 1. Hydrographic sections carried out in the Lesser Antilles passages during the ship cruises between 2002 and 2005 (red) with additional sections done in September 2005 (yellow). Names of passages used in the text are given and the islands of Tobago and Puerto Rico are labeled.

warm water from the South Atlantic ($\sigma_\theta < 27.1$ kg m^{-3}) and reported a mean SAW transport of 9.1 Sv into the Caribbean. The intermediate SAW flow is however dominated by NBC rings, which remain in the Atlantic. The total estimated northward SAW transport was 5.3 Sv at 16°N.

[5] Here we extend these results by new measurements from September 2005 to provide a comprehensive account of the Caribbean inflow (total and SAW) through the Lesser Antilles Passages, and we compare the results to a high-resolution Atlantic Ocean model of the wind-driven and thermohaline circulation. We use the model simulation to further examine the origin of the Caribbean inflow and the pathways of SAW.

[6] We use a water mass analysis to distinguish SAW from water originating in the northern hemisphere, an approach that has been widely used in the past [e.g. *Schmitz and Richardson*, 1991; *Schmitz and McCartney*, 1993; *Poole and Tomczak*, 1999; *Johns et al.*, 2003; *Garraffo et al.*, 2003; *Rhein et al.*, 2005]. Hereby it is not possible to identify that part of the SAW which gets transformed in the tropical and subtropical cells and is transported into our study region and consequently this SAW transport is partly missing in our estimates. At least in the model simulations analyzed here, the missing part turned out to be small (see Discussion).

2. Data and Model Experiments

[7] To investigate the Caribbean inflow, the passages between the Lesser Antilles were visited four times from 2002 to 2005. Details for the three repeats in 2002–2004 are given by *Rhein et al.* [2005]. During RV METEOR cruise M66/1 (September 2005), the measurements were extended to the Antigua and Anegada passages north of Guadeloupe (cf. Figure 1). The CTD accuracy for all cruises (including M66/1) was 0.002–0.003°C for temperature and 0.002–0.003 for salinity. A 38 kHz and a 75 kHz vessel mounted ADCP (RD Instruments) were used in September 2005 with a vertical range of 1400 m, covering all water masses relevant for this study. Like for the former cruises, the accuracy of the hourly averaged horizontal velocities was 0.05 ms^{-1}. The resulting error in the transport calculations is less than 0.1 Sv.

[8] The data analysis is complemented by a high-resolution ocean model simulation, utilizing the primitive equation model that has been developed for studying the wind-driven and thermohaline circulation in the Atlantic Ocean (Family of Linked Atlantic Model Experiments, FLAME) [*Dengg et al.*, 1999]. The FLAME hierarchy of models are based on a modified version of the z-coordinate, Modular Ocean Model (MOM2) [*Pacanowski*, 1995]. The simulation considered here uses a horizontal grid of $\frac{1}{12}$° and 45 vertical levels, for a domain from 70°N to 18°S [cf. *Eden and Böning*, 2002; *Böning et al.*, 2006]. The model is forced with monthly-mean wind stresses and heat fluxes based on a climatology of the European Centre for Medium Range Forecasts (ECMWF) analysis following *Barnier et al.* [1995] and the DYNAMO study [*Willebrand et al.*, 2001]. Sea surface salinity, as well as the hydrographic conditions at the closed northern, and for the inflow through the open southern boundaries are damped toward climatological values. The model bathymetry was not fine tuned for the purpose of this study, and thus lacks some detail in the area of the Antilles passages (e.g., missing some of the deep parts); all passages are nevertheless represented in the model (see Figures 4 and 5). The model has been integrated for 15 years; here we present results based on monthly mean fields from the last year of integration. A later run with interannual variability in the forcing was used to compare to the climatological run.

[9] For the calculation of the SAW fractions, an isopycnal mixing approach is applied following *Rhein et al.* [2005]. One source represents the northern waters (18°N/55°W, 24°N/50°W), the other is placed in the southern hemisphere (10°S/35°W, 3°S/23°W), corresponding to the main upstream sources for the Caribbean inflow waters. For the observations, the source water characteristics were taken from historical data, and for the model extracted from the climatological run at nearly identical positions. The modeled and observed source waters are shown in Figure 2 (blue: model; red: observations). The observed and modeled water masses agree particularly well in the central waters, while the model is slightly saltier in the intermediate waters. The salinity maximum waters are recognizable in the model, but the property differences between the sources are somewhat smaller than observed. Since the model simulates the

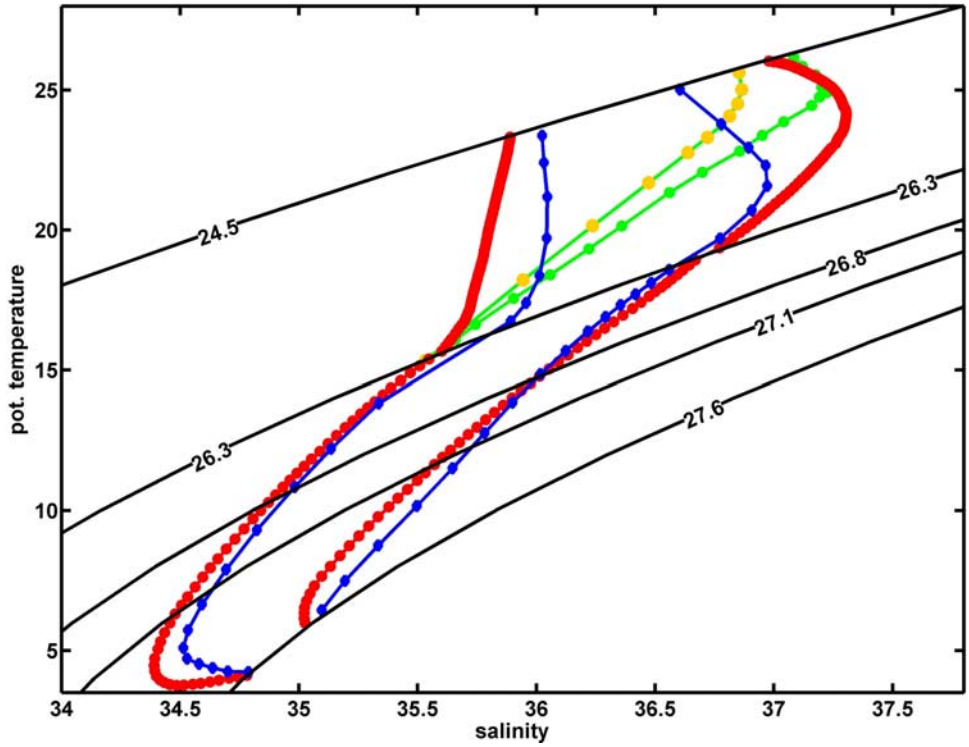

Figure 2. Source water profiles used for the T/S analysis. One source represents the northern waters (18°N/55°W, 24°N/50°W) and appears on the right side of the T/S diagram. The other source is placed in the southern hemisphere (10°S/35°W, 3°S/23°W) and fresher than the northern source, thus located on the left side in the T/S diagram. The red profiles illustrate the observational sources and the blue profiles were extracted from the model. The shorter green lines represent the salty South Atlantic source (green data points: observed profile; yellow data points: modeled profile).

observed water masses satisfyingly, the same separating isopycnals are used as in the observational analysis. As mentioned above, some SAW is modified, partly upwelled and transformed in its properties in the tropical/subtropical cells [*Schott et al.*, 2004]. The upwelled SAW is partly transported back to the western boundary and enters the northern hemisphere with the NBC. This transformed SAW thus contributes to the surface layer and is accounted for in the transport estimates, since all surface water is assumed to be of southern hemispheric origin. Some of the transformed water nevertheless remains in the Atlantic and is transported northwestward in the Ekman layer, e.g., as can be seen in an analysis of surface drifter data [*Grodsky and Carton*, 2002]. Its contribution to the SAW transport is missed. An estimate is given in the Discussion.

[10] The separation into four different water masses was adopted from *Rhein et al.* [2005]: Surface water (SW: $\sigma_\theta < 24.5$ kg m^{-3}) is thought to be of South Atlantic origin south of Guadeloupe [*Schmitz and Richardson*, 1991; *Rhein et al.*, 2005] and entirely of North Atlantic origin north of Guadeloupe. We drew the line to the North Atlantic regime here, because the salinity minimum of the Amazon plume has faded near Guadeloupe (the mean surface salinity is >35 psu there), and the Chlorophyll a distribution [e.g., *Signorini et al.*, 1999] indicates Amazon and Orinoco influence in all the Caribbean Sea area, but not at the northern Atlantic side (e.g., north of Puerto Rico). Some surviving NBC rings might carry surface waters from the South Atlantic to latitudes north of 16°N. If some of these rings enter the Caribbean through Antigua and Anegada Passage, this surface SAW will be missed in our estimates.

[11] Below the mixed layer, a distinctive salinity maximum identifies the Salinity Maximum Water (SMW). The salinity maximum is found at approximately 100–120 m in the Lesser Antilles region and reaches peak values of more than 37 psu. The density layer σ_θ = 24.5–26.3 kg m^{-3}, which spans about 100 m, embeds the maximum. A separation of the two salty northern and southern sources is difficult due to similar properties. In the southeastern Atlantic a fresher variety of this water mass occupies the density range [*Wilson et al.*, 1994] and is brought westward with the SEC. In our water mass analysis we use only the fresher southeastern Atlantic source. This problem is evident in both the model and the observations. To illustrate this problem, the salty South Atlantic source is included in Figure 2 (green). To estimate the contribution of both South Atlantic water masses, float trajectories have been analyzed (see Results).

[12] The Central Water (CW: σ_θ = 26.3 – 27.1 kg m^{-3}) located in about 200–500 m depth is separated in an upper CW and a lower CW by the isopycnal σ_θ = 26.8 kg m^{-3}. The deepest layer analyzed is the Intermediate Water (IW), bounded by the isopycnal σ_θ = 27.6 kg m^{-3}, located at approximately 1100 m. The choice of the source waters and the assumption of isopycnal mixing lead to errors of ±12% in the IW layer fractions and of ±6% in the CW layers. The

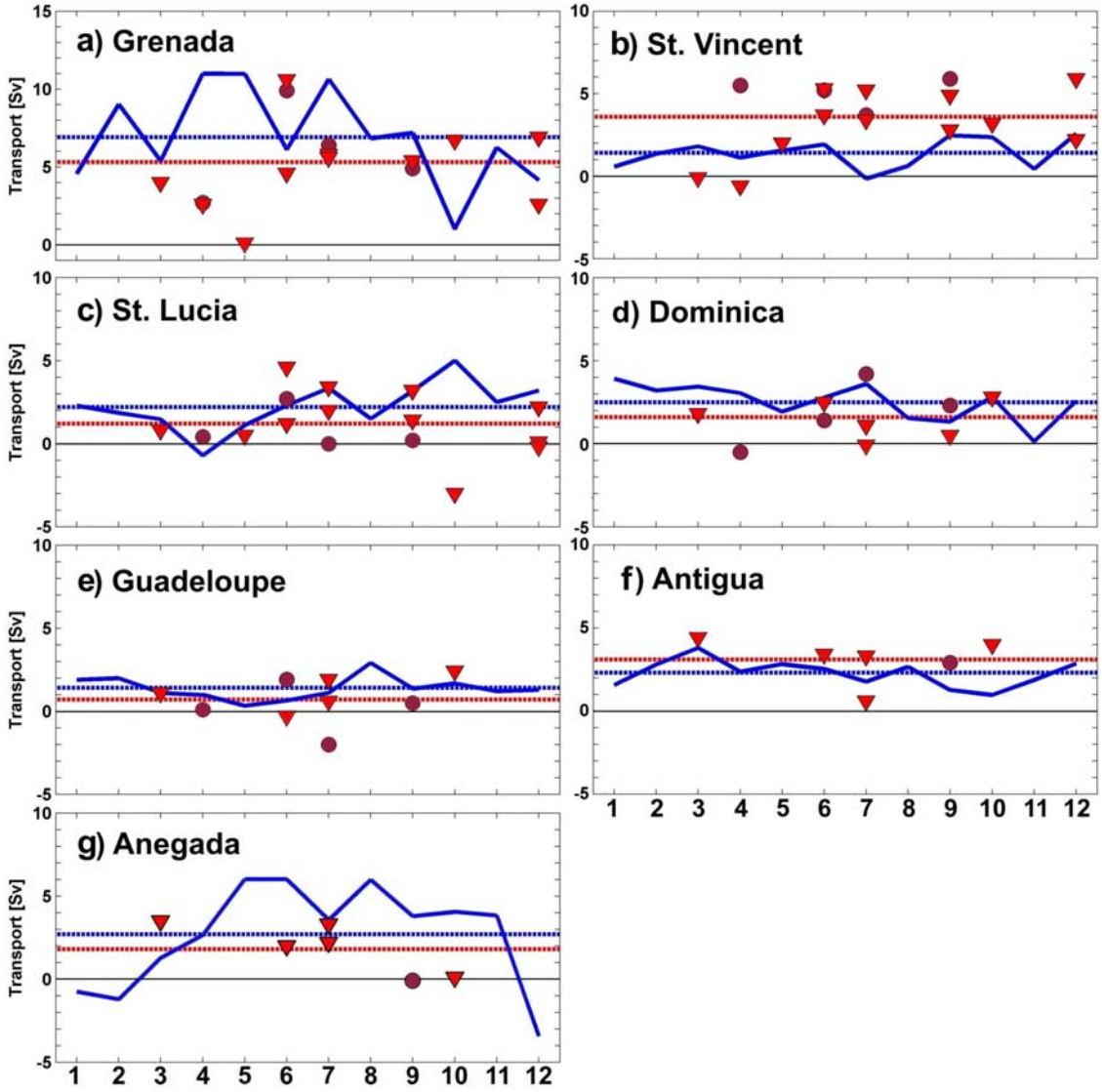

Figure 3. Observed (1991–2005) and modeled transports with mean value (dashed lines) into the Caribbean Sea through the passages between Tobago and Puerto Rico. Blue: results from the FLAME model (climatological run), red: observed inflow, where triangles are the transports from *Johns et al.* [2002] and darker circles the transports from our cruises. The transports (in Sv) are plotted against the month of observation/simulation. Note the different transport scale of Figure 3a.

error in the SMW is clearly higher, due to the neglected western saline South Atlantic source [*Rhein et al.*, 2005].

[13] Water mass transports are calculated from gridded ADCP and CTD data. The vertical resolution is 10 m, the horizontal resolution 7.5 nm in Grenada Passage, 0.4 nm in the passages from Guadeloupe to St. Vincent, and 0.7 nm in Antigua and Anegada Passage. The error from the data interpolation was negligible. The tides in the passages were removed by averaging over multiple ADCP repeats during each cruise. The SAW transports were derived by multiplying the passage velocity with the corresponding SAW fraction at each grid point and then integration over the passage. The transport at the shallow section (<200 m depth) between Antigua and Anegada passage was negligible (0.04 Sv) during September 2005.

[14] The high resolution FLAME model represents the Lesser Antilles Passages well, with at least three horizontal grid points in velocity and more in temperature and salinity in the narrow passages. To calculate the SAW transport, temperature and salinity are interpolated to the velocity grid.

Table 1. Mean Inflow Into the Caribbean (in Sv) Through the Lesser Antilles Passages From All Data Shown in Figure 3[a]

	Observations	Model
Grenada	5.3 ± 2.8 (0.8)	6.9 ± 3.1 (0.9)
St. Vincent	3.6 ± 2.0 (0.5)	1.4 ± 0.9 (0.3)
St. Lucia	1.2 ± 1.8 (0.5)	2.2 ± 1.4 (0.4)
Dominica	1.6 ± 1.4 (0.5)	2.5 ± 1.1 (0.3)
Guadeloupe	0.7 ± 1.4 (0.5)	1.4 ± 0.7 (0.2)
Antigua	3.1 ± 1.3 (0.6)	2.3 ± 0.8 (0.2)
Anegada	1.8 ± 1.5 (0.7)	2.7 ± 3.1 (0.9)
Total	17.3 ± 4.8 (1.5)	19.4 ± 4.9 (1.4)

[a]Observations versus model (annual mean) with standard deviation and standard error in parenthesis.

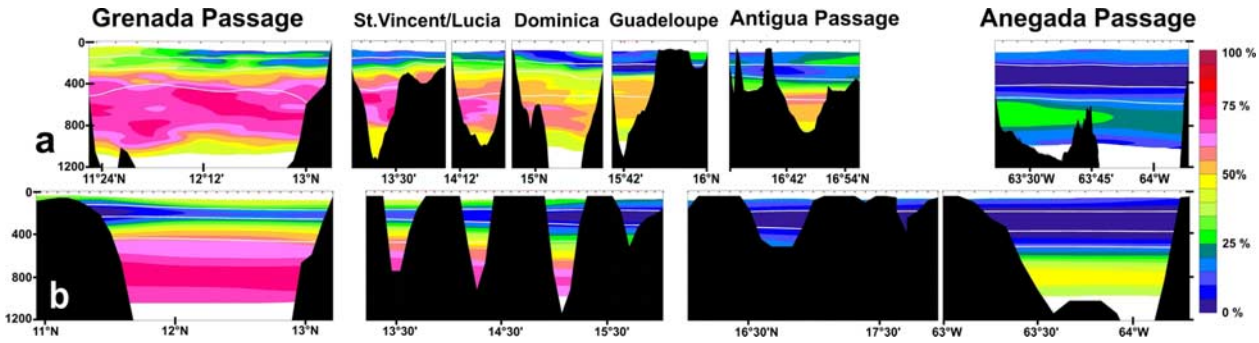

Figure 4. (a) South Atlantic Water distribution (in %) during the cruise in September 2005 and (b) mean SAW distribution in the FLAME model. The passages are shown from Tobago on the left going northward to Puerto Rico. The passage width shown is proportional, except for Anegada Passage (twice as wide). The topography is derived either from echo sounder data or the model grid. The water masses and their separating densities are (1) SMW from 24.4 kg m^{-3} to 26.3 kg m^{-3}, (2) UCW from 26.3 kg m^{-3} to 26.8 kg m^{-3}, (3) LCW from 26.8 kg m^{-3} to 27.1 kg m^{-3}, (4) IW from 27.1 kg m^{-3} to 27.6 kg m^{-3}.

In the vertical, the model has 45 layers (27 of them above 1200 m), while near the surface, the resolution reaches 10 m and decreases smoothly downward. Thus, all water masses are always existent. The differences between the real and the model topography are rather small as can be realized by comparing Figures 1 and 5 or in Figure 4.

3. Results

3.1. Total Inflow

[15] In Figure 3 the monthly mean transports from the model (blue) are compared with all available historical shipboard data in the respective month [*Johns et al.*, 2002; *Rhein et al.*, 2005] and the new results from September 2005 (red). The monthly mean transports of the climatological year are comparable to the ones of a 15-year time series with interannual variability in the forcing (not shown). The annual means (and standard deviations) of both runs are similar for the Caribbean inflow (19.4 Sv ± 4.9 Sv versus 19.6 Sv ± 4.8 Sv, respectively, see below). The climatological year can thus be considered representative of the model.

[16] In contrast, the observed data represent single day snapshots of the passage transports, collected over many years. Large variability can occur, and in the case of Grenada Passage the minimum transport ever measured (May) is directly followed by the maximum in the next month (June). But during one month, large variability is possible as well, e.g., in Grenada Passage in June: the single observations differ up to 5 Sv. Hence, the inflow through the passages is clearly influenced by mesoscale variability, probably caused by NBC rings, which lead to varying situations in the different years. The model reproduces the range of variability in Grenada Passage, but provides a higher mean inflow. Especially during the first months of the year, the model apparently produces higher transports than observed. This stronger inflow is partly compensated by smaller inflow through St. Vincent Passage. The differences occurring in these two passages might result from the somewhat simplified bathymetry in the model; Grenada Passage throughflow is favored over St. Vincent Passage flow in FLAME.

[17] The mean model transports (blue dotted) exceed the observed mean (red dotted) in all passages but St. Vincent and Antigua (Table 1). The transports are strongest through Grenada Passage and weakest through Guadeloupe Passage in both model and observations. Occasional outflow occurs, but the mean transports are always into the Caribbean. The standard deviations of the means are large, sometimes larger than the mean itself. The range of variability indicated by this is reproduced in the model; the ranges overlap in all passages except in St. Vincent Passage. One should note, that observations in winter are sparse or missing. The study by *Johns et al.* [2002] finds an inflow through the Lesser

Table 2. Mean SAW Inflow Into the Caribbean (in Sv) Through the Passages South of Guadeloupe During Our Observations[a]

	SW + SMW	CW	IW	SAW Frac
Grenada	2.1 ± 0.4 (0.2)	1.0 ± 0.6 (0.3)	0.6 ± 1.5 (0.7)	48% ± 16%
St. Vincent	2.8 ± 0.9 (0.5)	0.6 ± 0.3 (0.1)	0.2 ± 0.5 (0.3)	44% ± 18%
St. Lucia	0.8 ± 0.4 (0.2)	0.0 ± 0.2 (0.1)	−0.2 ± 0.3 (0.2)	42% ± 16%
Dominica	0.2 ± 1.1 (0.6)	0.2 ± 0.1 (0.1)	0.2 ± 0.4 (0.2)	31% ± 18%
Guadeloupe	0.1 ± 0.5 (0.3)	0.1 ± 0.2 (0.1)	−0.1 ± 0.1 (0.1)	28% ± 18%
Total	6.0 ± 1.6 (0.4)	1.7 ± 0.7 (0.3)	0.7 ± 1.6 (0.9)	

[a]The standard deviation is given, as well as the standard error in parenthesis. Differences to the total are due to rounding. The mean SAW fraction for σ_θ = 24.5 − 27.6 kg m^{-3} is provided for each passage in the last column.

Table 3. Same as Table 2 but for the Model Months April–September

	SW + SMW	CW	IW	SAW Frac
Grenada	5.7 ± 1.3 (0.5)	0.4 ± 0.2 (0.1)	0.3 ± 0.2 (0.1)	42% ± 23%
St. Vincent	−0.2 ± 0.5 (0.2)	0.3 ± 0.1 (0.1)	0.3 ± 0.1 (0.1)	43% ± 22%
St. Lucia	−0.3 ± 0.6 (0.2)	0.2 ± 0.2 (0.1)	0.7 ± 0.2 (0.1)	38% ± 22%
Dominica	0.3 ± 0.4 (0.2)	0.1 ± 0.1 (0.1)	0.2 ± 0.2 (0.1)	26% ± 20%
Guadeloupe	0.4 ± 0.6 (0.2)	0.1 ± 0.1 (0.1)	0.0 ± 0.0	16% ± 12%
Total	5.9 ± 1.6 (0.7)	1.1 ± 0.3 (0.1)	1.5 ± 0.3 (0.1)	

Antilles passages of 18.4 Sv ± 4.7 Sv in observations, when adding our cruises, the inflow decreases slightly to 17.3 Sv ± 4.8 Sv. Their model with a $\frac{1}{3}^\circ$ resolution and 6 vertical layers showed an inflow of 21.7 Sv, while we find 19.4 Sv in FLAME, which is somewhat closer to the observations.

3.2. SAW Fractions

[18] The SAW distribution from September 2005 (Figure 4a) shows similar features as the earlier measurements in the work of *Rhein et al.* [2005, Figure 4]. The SAW fractions are highest in Grenada Passage and decrease toward the northern passages. The IW layer shows the highest SAW influence, while the lowest is found in the UCW layer. The FLAME model reproduces this partitioning. Differences between the model and the observations include the following:

[19] 1. The major difference occurs in Guadeloupe Passage, where the mean SAW fraction is 16% in FLAME and 30% in the observations.

[20] 2. Antigua Passage differs as well and the reason for this discrepancies is most likely the smoothed model topography, erasing the passages below approximately 450 m depth.

[21] 3. The contribution of South Atlantic IW in the Anegada passage is significantly higher in the model (38%) than in the data (21%).

[22] 4. In the four southern passages (Grenada to Dominica Passage), the modeled SAW fractions are higher in the SMW than the observed ones by at least 10%.

[23] 5. The upper CW contains less SAW in the model than in the observations. This is in good agreement with the older findings by *Schmitz and Richardson* [1991], as our UCW layer corresponds roughly to their 12°–24°C water, in which they presume only 5% SAW in the Florida Current as nearly all volume of this water mass is assumed to recirculate into the North Equatorial Undercurrent. This SAW loss by retroflection seems to be higher in the model than in our observations.

[24] The mean SAW fractions summed over all passages (from Guadeloupe) during our cruises vary mostly in the SMW layer: here, fractions from 17% to 35% occur. In the UCW layer the fractions are between 15% and 27%, while below the variability abruptly decreases: only 44%–53% in the LCW and 56%–59% in the IW. In the model the annual mean SAW fractions from Guadeloupe to Tobago are 40% in SMW, only 6% in UCW, 30% in LCW, and 62% in IW.

3.3. SAW Transports

[25] To compare with the shipboard data, SAW transports in the FLAME model are calculated both for (1) April to September, to coincide with the period of the cruises, and (2) the annual mean. We first describe the results for the April–September period. The modeled and observed SAW transports for the passages are summarized in Tables 2 and 3. The model and observations agree well on the total SAW transport (8.4 Sv and 8.5 Sv). Both show similar small total SAW transports through the Guadeloupe (obs. 0.1 Sv; mod. 0.5 Sv), Dominica (0.6 Sv), and St. Lucia (0.6 Sv) passages. The two other modeled passages differ from the observations. In the model, the SAW transport through Grenada passage is dominated by SW/SMW with minor contributions of the central and intermediate water masses while in the observations, the transports are more equally distributed. This discrepancy between model and data is compensated by the flow through St. Vincent passage: In the model, the SW/SMW transport is weak (0.4 Sv), while 2.8 Sv were found in the observations.

[26] Across all the passages, a SAW inflow of 6.0 Sv was observed for the upper two layers combined (SW and SMW), similar to the model value of 5.9 Sv. The CW inflow is weak in model and data (1.1 Sv and 1.7 Sv, respectively), caused by very low SAW contributions in the upper Central Water (see above). The Intermediate water inflow is 1.5 Sv in the model and 0.7 Sv in the observations. The observed total SAW inflow into the Caribbean south of Guadeloupe (8.5 Sv ± 2.4 Sv) is very nearly replicated by the model (8.4 Sv ± 1.7 Sv) in the months April to September.

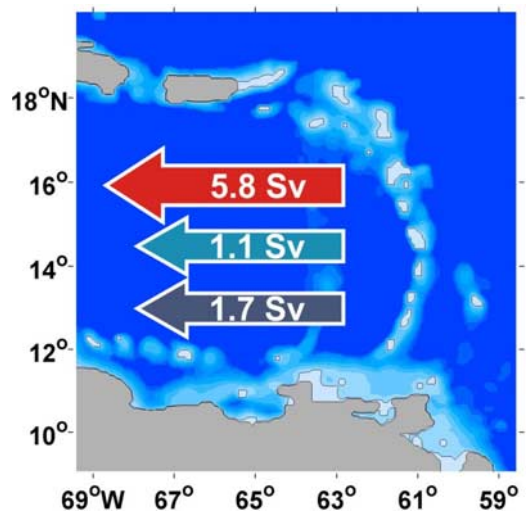

Figure 5. Annual South Atlantic Water transport into the Caribbean Sea in FLAME through the Lesser Antilles passages (Tobago–Puerto Rico). The underlaying topography was derived from the model u,v grid. Red: surface water + SMW, light blue: CW, dark blue: IW.

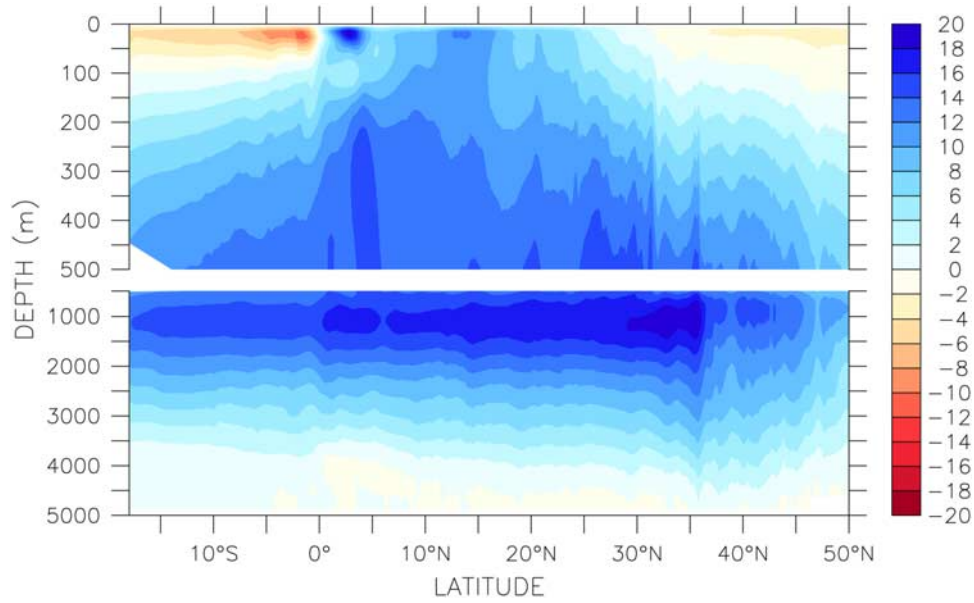

Figure 6. Mean overturning stream function (in Sv) in the FLAME model (climatological forcing). Note the different scale for the upper 500 m of the water column.

[27] For the annual mean, these modeling results do not change much. The only significant difference occurs in Grenada Passage, where the SW/SMW inflow drops to 4.3 Sv. This is 1.4 Sv less than in the summer months. A compensation occurs partly in St. Vincent and St. Lucia passages, where the outflow is reduced to −0.1 Sv in St. Vincent Passage and St. Lucia Passage turns to 0.1 Sv inflow. A slightly strengthened inflow in Dominica Passage (0.4 Sv) leads to the total SW/SMW inflow of 5.1 Sv in the annual mean. The other layers stay about the same with 1.0 Sv inflow in CW and 1.4 Sv in IW. These layer transports sum up to a total annual mean inflow of 7.5 Sv (±1.3 Sv).

[28] The comparison of the SAW transports through the passages north of Guadeloupe depends on the single observation from September 2005 (not shown in Table 2). The observed SAW flow into the Caribbean was zero through Anegada passage and 0.6 Sv through Antigua Passage. In the model, Antigua Passage yields 0.1 Sv SAW inflow and Anegada Passage 0.4 Sv inflow in the annual mean (occurring mostly in the IW layer). The low transports through Antigua Passage in the model originate from the model topography: the passage is very shallow and does not contain any IW. The sum of the transports through the northern passages was comparable in the observations and the model.

4. Discussion

[29] In this article, we compare shipboard observations, which represent single day-snapshots in transports and water masses, with climatological monthly mean model results. Although the model has a high resolution, the model bathymetry is simplified and might be the cause of disagreements with the observations. After all, the model reproduces reasonably well the observed total inflow and the observed total SAW inflow, as well as the water mass distribution. While differences in the individual passages occur (especially in St. Vincent Passage), the overall inflow into the Caribbean is convincingly achieved by the model simulation.

[30] The seasonal cycle is unresolved in both model and observations. Since the climatological year represents a mean state of the current field, one would expect a strong seasonal cycle to be apparent in the climatological year as well. We suggest that the seasonal cycle in FLAME is thus small and the variability rather occurs on 1–3 months time scales. The model study of *Johns et al.* [2002] found strong seasonal variations in Grenada and St. Vincent passages. This behavior could not be reproduced in FLAME so far, but the 15-year time series with interannual variability in the forcing should be useful for a further investigation on that topic. The modeled passage transports fit into the range of the observed variability, where even measurements taken in the same month in different years show large discrepancies.

[31] As already mentioned, the SMW consists of three sources: a saline northern source, a saline southwestern source and a fresh southeastern source. In our T/S analysis we use only the eastern source to calculate the SAW contribution. On the basis of the geostrophic flow maps from *Zhang et al.* [2003], *Rhein et al.* [2005] estimated an additional SAW contribution from the southwestern source of 1.9 Sv. We applied the isopycnic T/S analysis to CTD and ARGO float data in the area between 5°S and 7°N and from the Brazilian coast to 40°W. The fraction of the fresh eastern SA source exceeded 70–75% throughout the year, leaving at maximum 25–30% from the southwestern SMW source. To obtain an upper estimate of the missing SAW transport from the southwestern source, we apply this ratio to the inflow of eastern South Atlantic SMW of 1.0 Sv, resulting in an inflow of the southwestern SAW source of 0.4 Sv. One should note, that data on the Brazilian shelf are missing and the shallow coastal flow might contain higher fractions of the southwestern source than found farther offshore. The observed mean SAW inflow including the

southwestern SMW source and the transport through Antigua and Anegada passages (0.6 Sv) sum up to 9.3 Sv.

[32] In the model, we introduced artificial floats in the Caribbean inflow region in the SMW layer and followed their trajectories backward for 3 years. The floats originating from the South Atlantic were separated into eastern and western types. In the model, the eastern South Atlantic source is also clearly more important than the western. A ratio of 1:3, western against eastern source, is obtained in the float experiment. This ratio is not much different from the calculated one above, obtained from ARGO floats. The annual mean modeled SMW inflow is 1.6 Sv, which is now supplemented by 0.6 Sv from the southwestern source.

[33] The discussed similarities between the model results in the summer month and the observations strengthen our confidence into the annual mean modeled SAW inflow. Including the SMW contribution from the saline southwestern source and the SAW transports through Antigua and Anegada passages, results in 8.6 Sv (annual mean) SAW entering the Caribbean in the model (Figure 5). This is close to the observed mean SAW inflow of 9.3 Sv. The model validation done here gives now strong indications, that the mean SAW transport of 8.6 Sv obtained is a good estimate for the direct western boundary pathway of MOC transport.

[34] The Antigua and Anegada passages turned out to be of minor importance for the SAW inflow into the Caribbean in the observations (0.6 Sv) and in the model (0.5 Sv). *Rhein et al.* [2005] reported 5.3 Sv SAW crossing 16°N in the Atlantic in NBC rings. Only 10–11% of that transport seem to enter the Caribbean and further investigations of the fate of this northward SAW transport is necessary. Either the rings enter the Caribbean only rarely through the northern passages, or the water mass properties were rapidly changed north of Guadeloupe, so that our analysis cannot identify the SAW any longer.

[35] The overturning stream function in FLAME amounts 16 Sv in the tropical region (Figure 6), transporting deep water southward. Subtracting 1 Sv of northward bottom water flow, the warm northward MOC transport has the order of 15 Sv in the model. 11 Sv occur in the surface and central water layers, and 4 Sv in the intermediate layer [cf. *Hüttl and Böning*, 2006, Figure 1c]. Our calculated Caribbean SAW inflow of 8.6 Sv thus achieves 63% of the overturning water with densities <27.1 kg m^{-3} and 41% of the IW. Now we reach the same conclusion as *Rhein et al.* [2005]: the main pathway for the upper and central waters is the Caribbean, while the major part of the intermediate water remains in the Atlantic. For the SAW remaining in the Atlantic, float trajectories in the model (not shown) indicate other pathways for SAW, an important one of them is connected to the NBC rings as observed [*Goni and Johns*, 2003].

[36] If we adopt the 5.3 Sv ring transport from *Rhein et al.* [2005] as the mean northward Atlantic flow at Guadeloupe, and add this to the SAW inflow through the Caribbean passages, a sum of 13.4 Sv is obtained. Given the strength of the warm northward MOC is 15 Sv as in the FLAME model, the water mass analysis identified about 90% of the MOC. The SAW portion taking the pathway via the EUC and equatorial upwelling regions must then be small, max. 1.7 Sv. Trajectories in the model show a possible pathway along the equator and northward near the Mid-Atlantic ridge. The exact position and strength of the interior Atlantic pathway and the fate of the NBC rings are topics for further investigations.

[37] **Acknowledgments.** We thank the Deutsche Bundesministerium für Bildung und Forschung (BMBF) and the Deutsche Forschungsgemeinschaft (DFG) for financial support. We acknowledge the contributions of J. Dengg, R. Redler, J.-O. Beismann, C. Eden, and L. Czeschel to the FLAME development and integration. The computations were performed at DKRZ, Hamburg.

References

Baklouti, M., J.-L. Devenon, A. Bourret, J.-M. Froidefond, J.-F. Ternon, and J.-L. Fuda (2007), New insights in the French Guiana continental shelf circulation and ints relation to the North Brazil Current retroflection, *J. Geophys. Res.*, *112*, C02023, doi:10.1029/2006JC003520.

Barnier, B., L. Siefridt, and P. Marchesiello (1995), Thermal forcing for a global ocean circulation model using a three-year climatology of ECMWF analysis, *J. Mar. Syst.*, *6*, 363–380.

Böning, C. W., M. Scheinert, J. Dengg, A. Biastoch, and A. Funk (2006), Decadal variability of subpolar gyre transport and its reverberation in the North Atlantic overturning, *Geophys. Res. Lett.*, *33*, L21S01, doi:10.1029/2006GL026906.

Dengg, J., C. W. Böning, U. Ernst, R. Redler, and A. Beckmann (1999), Effects of an improved model representation of overflow water on the subpolar North Atlantic, *Int. WOCE Newsl.*, *37*, 10–15.

Eden, C., and C. W. Böning (2002), Sources of eddy kinetic energy in the Labrador Sea, *J. Phys. Oceanogr.*, *32*, 3346–3363.

Fratantoni, D., and D. Glickson (2002), North Brazil Current Ring generation and evolution observed with SeaWiFS, *J. Phys. Oceanogr.*, *32*, 1058–1074.

Garraffo, Z. D., W. E. Johns, E. P. Chassignet, and G. J. Goni (2003), North Brazil Current rings and transport of southern waters in a high resolution numerical simulation of the North Atlantic, in *Interhemispheric Water Exchange in the Atlantic Ocean*, *Elsevier Oceanogr. Ser.*, vol. 68, edited by G. J. Goni and P. Malanotte-Rizzoli, pp. 335–356, Elsevier, New York.

Goni, G. J., and W. E. Johns (2003), Synoptic study of warm rings in the North Brazil Current retroflection region using satellite altimetry, in *Interhemispheric Water Exchange in the Atlantic Ocean*, *Elsevier Oceanogr. Ser.*, vol. 68, edited by G. J. Goni and P. Malanotte-Rizzoli, pp. 335–356, Elsevier, New York.

Grodsky, S. A., and J. A. Carton (2002), Surface drifter pathways originating in the equatorial Atlantic cold tongue, *Geophys. Res. Lett.*, *29*(23), 2147, doi:10.1029/2002GL015788.

Hüttl, S., and C. W. Böning (2006), Mechanisms of decadal variability in the shallow subtropical-tropical circulation of the Atlantic Ocean: A model study, *J. Geophys. Res.*, *111*, C07011, doi:10.1029/2005JC003414.

Johns, W. E., T. L. Townsend, D. M. Fratantoni, and W. D. Wilson (2002), On the Atlantic inflow to the Caribbean Sea, *Deep Sea Res. I*, *49*, 211–243.

Johns, W. E., R. J. Zantopp, and G. J. Goni (2003), Cross-gyre transport by North Brazil Current rings, in *Interhemispheric Water Exchange in the Atlantic Ocean*, *Elsevier Oceanogr. Ser.*, vol. 68, edited by G. J. Goni and P. Malanotte-Rizzoli, pp. 411–436, Elsevier, New York.

Lumpkin, R., and S. L. Garzoli (2005), Near-surface circulation in the Tropical Atlantic Ocean, *Deep Sea Res. I*, *52*, 495–518.

Lux, M., H. Mercier, and M. Arhan (2001), Interhemispheric exchanges of mass and heat in the Atlantic Ocean in January–March 1993, *Deep Sea Res. I*, *48*, 605–638.

Pacanowski, R. (1995), MOM2 documentation, users guide and reference manual, *Tech. Rep. 3*, 329 pp., Geophys. Fluid Dyn. Lab., Princeton, N. J.

Poole, R., and M. Tomczak (1999), Optimum multiparameter analysis of the water mass structure in the Atlantic Ocean thermocline, *Deep Sea Res. I*, *46*, 1895–1921.

Rhein, M., K. Kirchner, C. Mertens, R. Steinfeldt, M. Walter, and U. Fleischmann-Wischnath (2005), Transport of South Atlantic Water through the passages south of Guadeloupe and across 16°N, 2000–2004, *Deep Sea Res. I*, *52*, 2234–2249.

Schmitz, W. J., Jr., and M. S. McCartney (1993), On the North Atlantic circulation, *Rev. Geophys.*, *31*, 29–49.

Schmitz, W. J., Jr., and P. L. Richardson (1991), On the sources of the Florida Current, *Deep Sea Res*, *38*, suppl. 1, S379–S409.

Schott, F. A., J. P. McCreary Jr., and G. C. Johnson (2004), Shallow overturning circulations of the tropical–subtropical oceans, in *Earth's Climate: The Ocean-Atmosphere Interaction*, *Elsevier Oceanogr. Ser.*, vol. 147, edited by C. Wang, S.-P. Xie, and J. A. Carton, pp. 261–304, Elsevier, New York.

Signorini, S. R., R. G. Murtugudde, C. R. McClain, J. R. Christian, J. Picaut, and A. J. Busalacchi (1999), Biological and physical signatures in the tropical and subtropical Atlantic, *J. Geophys. Res.*, *104*(C8), 18,367–18,382.

Snowden, D., and R. Molinari (2003), Subtropical cells in the Atlantic Ocean: An observational summary, in *Interhemispheric Water Exchange in the Atlantic Ocean*, *Elsevier Oceanogr. Ser.*, vol. 68, edited by G. J. Goni and P. Malanotte-Rizzoli, pp. 287–312, Elsevier, New York.

Willebrand, J., B. Barnier, C. W. Böning, C. Dieterich, P. D. Killworth, C. Le Provost, Y. Jia, J.-M. Molines, and A. L. New (2001), Circulation characteristics in three eddy-permitting models of the North Atlantic, *Progr. Oceanogr.*, *48*, 123–161.

Wilson, W. D., E. Johns, and R. L. Molinari (1994), Upper layer circulation in the western tropical North Atlantic Ocean during August 1989, *J. Geophys. Res.*, *99*(C1), 22,513–22,523.

Zhang, D., M. J. McPhaden, and W. E. Johns (2003), Observational evidence for flow between the subtropical and tropical Atlantic: The Atlantic subtropical cells, *J. Phys. Oceanogr.*, *33*, 1783–1797.

C. W. Böning, Leibniz Institut für Meereswissenschaften Düsternbrooker Weg 20, D-24105 Kiel, Germany.

S. Hüttl, K. Kirchner, C. Mertens, and M. Rhein, Institut für Umweltphysik, Universität Bremen, Postfach 330 440, D-28334 Bremen, Germany. (kkirchner@uni-bremen.de)